REPORT DOCUMENTATION PAGE

Form Approved
OMB NO. 0704-0188

1. AGENCY USE ONLY (Leave Blank)	2. REPORT DATE 04/02/2003	3. REPORT TYPE AND DATES COVERED Final, 06/01/2001 – 11/30/2002

4. TITLE AND SUBTITLE
Metachromatic Materials Final Progress Report

5. FUNDING NUMBERS
C: DAAD19-01-1-0598
PR: P-42187-PH-YIP-01108-1

6. AUTHOR(S)
P. Gregory Van Patten

7. PERFORMING ORGANIZATION NAME(S) AND ADDRESS(ES)
Ohio University
105 Research & Technology Ctr.
Athens, OH 45701

8. PERFORMING ORGANIZATION REPORT NUMBER PGVP-ARO-04022003

9. SPONSORING / MONITORING AGENCY NAME(S) AND ADDRESS(ES)
U. S. Army Research Office
P.O. Box 12211
Research Triangle Park, NC 27709-2211

10. SPONSORING / MONITORING AGENCY REPORT NUMBER
42187.3-PH-YIP

11. SUPPLEMENTARY NOTES
The views, opinions and/or findings contained in this report are those of the author(s) and should not be construed as an official Department of the Army position, policy or decision, unless so designated by other documentation.

12 a. DISTRIBUTION / AVAILABILITY STATEMENT
Approved for public release; distribution unlimited.

12 b. DISTRIBUTION CODE

13. ABSTRACT (Maximum 200 words)
This report details progress achieved under the contract designated above.

14. SUBJECT TERMS			15. NUMBER OF PAGES 17
			16. PRICE CODE
17. SECURITY CLASSIFICATION OR REPORT UNCLASSIFIED	18. SECURITY CLASSIFICATION ON THIS PAGE UNCLASSIFIED	19. SECURITY CLASSIFICATION OF ABSTRACT UNCLASSIFIED	20. LIMITATION OF ABSTRACT UL

FINAL PROGRESS REPORT—METACHROMATIC MATERIALS

1. Table of Contents

2. List of Appendixes, Illustrations and Tables

3. Statement of the Problem Studied

The primary goal of the work performed under this contract was to study the feasibility of using metal nanoparticles as contrast agents (ink) in full-color, flexible, reflective, low-power, electronic displays. The concept is based on the tunability of the plasmon absorption peak in metal nanoparticle ensembles. Well-separated, nanometer-sized fragments of Au, Ag, or Cu have intense plasmon absorptions in the visible part of the spectrum.[1-3] The extinction coefficient, ε, the frequency of maximum absorbance, ν_{max}, and the full width at half maximum, $\Delta\nu_{1/2}$, of the plasmon peak all depend on the sizes of the nanoparticles. As the nanoparticles increase in size from 2 to 20 nanometers, the peak becomes sharper and more intense (i.e. ε increases and $\Delta\nu_{1/2}$ decreases). The spectral position of the peak remains relatively unchanged over this size range. As particles are brought into close proximity—less than about 3 diameters between their respective centers—the position of the plasmon peak red-shifts, leading to a dramatic change in color. The magnitude of the shift and the color change is proportional to the extinction coefficient of the nanoparticles. Because larger particles have larger ε and smaller $\Delta\nu_{1/2}$, they are expected to be best-suited for metachromatic (color-changing) applications.

In order to prove the possibility of using this plasmon shift in an electronic display, we set out to develop a scheme to electrically control the distribution of (and distances between) metal nanoparticles in a soft or fluid matrix. We first observed a controllable, reversible plasmon shift in a solid matrix prior to the commencement of this contract, but the control mechanism in this case was not electronic.[4] In the Fall of 2000, we built a series of thin films containing dendrimer-encapsulated Ag nanoparticles. The films were fabricated by the layer-by-layer method using poly(acrylic acid) (PAA) and poly(amidoamine) (PAMAM)-encapsulated nanoparticles. When the pH and ionic strength of the dipping solutions were properly controlled, pale yellow films were obtained. Absorption spectra of these films showed a plasmon absorption peak characteristic of the Ag nanoparticles. Upon dipping into acidic solutions and drying under a stream of nitrogen, the films were observed to change to an orange, and eventually to a red hue. The absorption spectrum showed a concomitant shift in the plasmon absorption peak from a wavelength of about 420 nm to 480 nm.

The observation was explained by a shrinkage of the film due to dehydration following the dip in an acid solution. When ionized, PAA is extremely hydrophilic, and the films are

hygroscopic. Even under ambient conditions, the films are swelled with water. When the films are dipped into acid, the PAA is protonated. The protonated (uncharged) form is much less hydrophilic and readily loses trapped water to evaporation. The shrinkage was believed to result in a decrease in the inter-particle separation in these films, and this change in the interparticle separation was believed to cause the plasmon shift as described above. These observations and interpretations directly led to the project described herein.

4. Summary of the Most Important Results

Our earliest work under this contract was aimed at resolving some inconsistencies in the properties of PAMAM-encapsulated silver nanoparticles. The synthesis of these particles was highly irreproducible, and our ability to make well-behaved particles under certain conditions contradicted reports in the literature regarding the behavior of PAMAM-encapsulated Ag nanoparticles.[5-7] After a few months of work, we were able to master the synthetic difficulties associated with these particles and publish a detailed account of the importance of pH in the synthesis and stability of these nanoparticles.[8]

The aforementioned dendrimer-Ag nanocomposite work holds a particular significance for the present project. In this work it was demonstrated that electrostatic interactions between particles could be controlled in solution [via pH regulation], and that these interactions could prevent collapse of the particles into suspended flocs. At low pH (< 6), amine groups on the PAMAM dendrimers were mostly protonated, and the dendrimers were positively charged. Repulsive forces between the like-charged dendrimers prevented precipitation and yielded a stable solution with a light yellow hue characteristic of the surface plasmons in nanocrystalline Ag^0. When the pH was raised above 7, the dendrimer began to deprotonate. Under these conditions, electrostatic stabilization of the colloid was disfavored, and the particles aggregated. The aggregation was caused by weaker, shorter-range van der Waals forces that are unimportant when ionic interactions are present. The aggregate was a deep red color owing to strong dipole-mediated interactions between surface plasmons on neighboring particles. The importance of this work for the present project is that it shows that strong, long-range electrostatic interactions can be used to toggle the propensity for stabilized colloidal nanoparticles to aggregate and change color. The overall goal of this work has been to drive this type of process using a purely electrical stimulus.

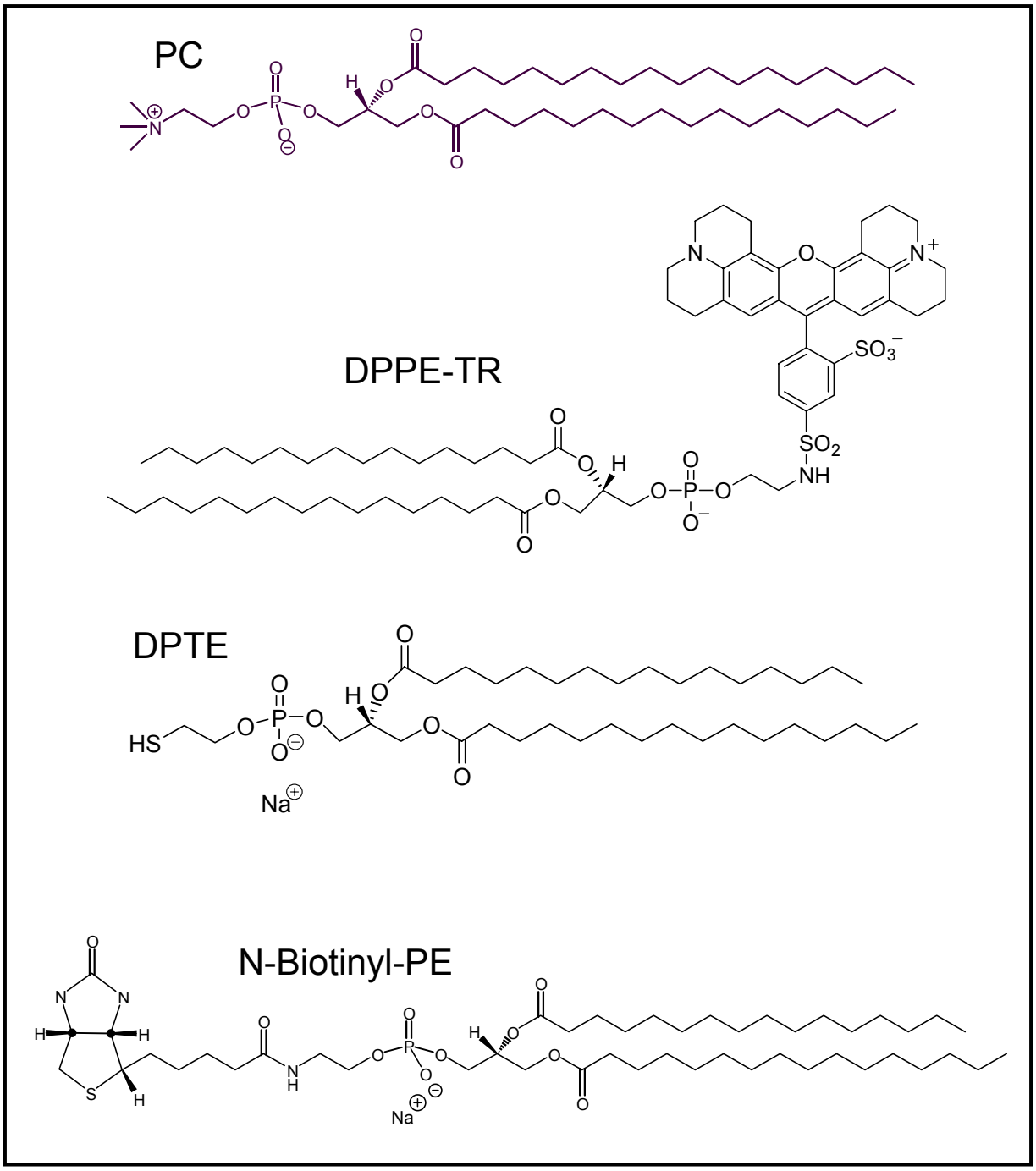

Chart 1. Structures of lipid molecules used in this work.

Following the completion of the work described above, we began to examine methods for electrically controlling the distribution and distances between individual nanoparticles in soft matrices. One of the most intriguing possibilities was the use of supported bilayer lipid membranes (BLMs) as two-dimensional fluids to confine the nanoparticles without completely eliminating their mobility. The inspiration for the work was drawn from previous studies by

Steven Boxer and co-workers at Stanford University several years earlier.[9,10] In their work, the Boxer group showed that BLMs could be patterned under certain conditions and that the patterning resulted in diffusional barriers to molecules attached to the membranes. Boxer and coworkers used lipids conjugated to fluorescent tags to observe migration across the individual BLMs. We began by reproducing these results within our laboratory.

4.1 Diffusion of Species Attached to Bilayer Lipid Membranes

We have fabricated BLMs from solutions of small unilamellar vesicles using established procedures.[9] Structures of the lipid molecules used in this work are shown in Chart 1. For the work using fluorescent tags, vesicles are formed from egg phosphatidylcholine (PC) and another lipid (DPPE-TR), present in smaller quantities whose hydrophilic headgroup has been labelled with Texas Red as a fluorophore. The vesicle solution is exposed to a clean, hydrophilic glass surface in the form of a microscope coverslip. Upon contacting the surface, the vesicles spontaneously lyse and fuse together to form a supported BLM structure on the glass. Another clean coverslip is placed atop the membrane to form a sandwich between two glass surfaces. In some cases, we have used tweezers to scratch lines in the BLMs. If the pH and ionic strength are properly controlled,[9] the edge of the membrane fuses together as the tweezers are drawn through. The result is a persistent gap of a few microns between two [now] separate membranes. Lipid molecules in the membrane are able to move freely in the plane of the membrane until they reach the gap. The gap acts as a diffusional barrier; molecules bound to the membrane cannot traverse the gap and move to the adjacent membrane.

Because the Texas Red-labelled lipid bears a net negative charge, it can be driven by an electric field (or electrophoretic flow) along the membrane. When these charged lipids reach the diffusional barrier, they stop and "pile up" along the edge of the membrane pad. We constructed a homemade electrophoresis cell in order to observe the migration of the Texas Red dye along the membrane under a fluorescence microscope. Typical fluorescence micrographs are shown in Figure 1. Figure 1(a) shows an individual membrane pad containing a small amount of DPPE-TR. Figure 1(b) shows the same membrane area after the application of a 50 V potential difference parallel to the membrane surface. The elapsed time was approximately 30 minutes between images. In image (b), the Texas Red fluorophore has congregated at the right hand edge of each individual membrane pad. This demonstrates the fluidity of the membrane and shows that it may be possible to use electrical manipulation to control the distribution of nanoparticles

across the membrane surface. By driving the nanoparticles against such a diffusional barrier, we could, in principle, change the distances between nanoparticles, and, perhaps, modulate the inter-particle electronic coupling enough to cause measurable shifts in the plasmon absorption peak.

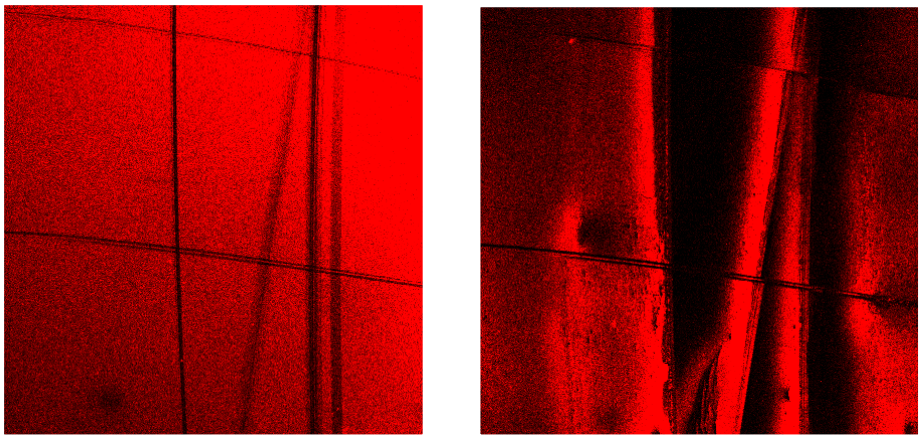

Figure 1. Fluorecence micrographs showing BLM labelled with DPPE-TR (a) before and (b) after application of a 50V potential gradient. Dark lines are scratches created with sharp tweezers. Elapsed time between images was 30 minutes.

Additional experiments were performed to probe the reversibility of the dye migration in the films. Figure 2 shows the same BLM area as Figure 1 following the reversal of the directionality of the applied 50 V potential gradient. The dye molecules can be seen to migrate and eventually congregate at the opposite edges of the membrane pads. Figure 3 shows the effect of turning off the applied field altogether. Brownian diffusion randomizes the distribution over time, and restores the homogeneity of the system.

Figure 2. Same as in Figure 1, following reversal of applied electric field for 30 min.

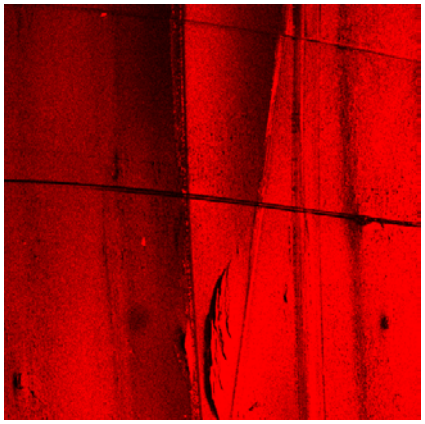

Figure 3. Same as in Figure 1, following removal of applied electric field for 70 min.

Several features of the BLM systems bear mention. First, the migration and congregation requires a relatively long time over the 0.1-1 mm distances shown in the figures above. This is due to the high viscosity of the BLM system and to the large distances being covered by the individual molecules. By reducing either the viscosity of the system or the scale of the membrane pads, the time response of the system can be correspondingly reduced. For example, reduction of the membrane size by a factor of 1000 (to 0.1-1 μm) should reduce the time response from tens of minutes to a few seconds. It should be easy to design an actual device based on electrophoresis that would be capable of response times of 1 second or less. Second, the congregation of the dye molecules affects most strongly those regions of the surface nearest the edges of the membrane pads. In Figure 1(b), the high dye concentration is seen only within a few tens of microns of the membrane edge. In order to maximize the effects of nanoparticle re-distribution (as observed over a macroscopic area), the density of these diffusional barriers would need to be maximized. In order to increase response rate and to increase the density of diffusional barriers, effort was devoted to the patterning of BLMs via stamping and blotting (see section 4.4 below).

4.2 BLMs and Metal Nanoparticles

The work on dye migration across BLMs suggested a novel way to electrically control the distances between nanoparticles. In order to use these BLMs as a model system to demonstrate the effect, it would be necessary to prepare a single layer of metal nanoparticles with an easily measurable absorbance. Using data obtained by Link and coworkers,[11] we can estimate the peak absorbance of a monolayer of metal nanoparticles. Measurements of the extinction coefficient of 20 nm Ag nanoparticles yielded values of approximately 9.8×10^{8} $M^{-1}\cdot cm^{-1}$ (where the concentration is given in terms of *particles*, rather than Ag atoms). Measurements on Au nanoparticles yielded values approximately half as large as those on Ag nanoparticles. If Beer's Law is assumed to be valid,

$$A = \varepsilon\, b\, c, \tag{1}$$

the measured absorbance of a sample of particles with extinction coefficient ε is determined by the product ($b\times c$), which describes the *area* density of particles within the interrogating beam path. If ε is given in traditional units of $M^{-1}\cdot cm^{-1}$, then the product ($b\times c$) simply represents the number of moles of particles found in an area of sample equal to 1 dm^3/cm, which is the same as

10 dm^2 or 1000 cm^2. Thus, if Beer's Law is extended to the case of a monolayer of particles on a surface, then the absorbance will be given by

$$A = [(1000\ cm^3/dm^3)\ \varepsilon\ \sigma]\ /N_A, \quad (2)$$

where σ is the surface density in particles per cm^2, N_A is Avogadro's number, and ε is the molar extinction coefficient expressed in conventional units ($M^{-1}\cdot cm^{-1}$). The maximum achievable surface density would result from a close-packed arrangement of spherical particles. Assuming a particle diameter of 20 nm, this leads to a surface density of 2.9×10^{11} particles/cm^2, and a calculated absorbance of 0.47 in the case of Ag nanoparticles or about 0.23 in the case of Au nanoparticles. From these considerations, we conclude that even with a relatively low fractional surface coverage of 5%, and using Au nanoparticles, we can expect a membrane absorbance of greater than 0.01. This optical density is easily within the range of values that can be reliably measured with conventional UV-Visible spectrometers. The spectrometer used in our work can readily achieve noise levels of 0.0001-0.0003 absorbance units over the spectral range of interest (300-700 nm).

4.3 Attaching Metal Nanoparticles to BLMs

After demonstrating electrophoretic migration of Texas Red across the membrane pads, efforts were made to attach metal nanoparticles to the lipid bilayers. The first scheme for effecting the attachment was based on the incorporation of thiolated lipids into the membranes. Attempts were made to attach silver nanoparticles to the membrane based on the well-known affinity of thiol groups for metallic Ag, Au, and Cu. A thiolated lipid, 1,2-dipalmitoyl-sn-glycero-3-phosphothioethanol (DPTE), was incorporated into vesicles consisting primarily of egg PC. Ag nanoparticles were prepared by borohydride reduction in aqueous solution in the presence of capping agents such as citrate or 3-mercaptopropanesulfonate. The nanoparticle solution was exposed to membranes containing DPTE or was combined with vesicle suspensions containing DPTE vesicles. No significant incorporation of metallic Ag into the BLM structure was observed. Alternatively, Ag nanoparticles were prepared with DPTE as a capping agent. The DPTE-stabilized particles were then exposed to membranes or vesicle suspensions comprised of a mixture of PC and DPTE. All of these efforts failed to yield membranes labelled with Ag nanoparticles. In the former case, the Ag-lipid conjugates apparently failed to insert into the established membrane; in the latter case, the Ag-lipid complexes precipitated from solution.

Following the failures with DPTE-stabilized nanoparticles, a new strategy was adopted. In this scheme, a biotinylated lipid—N-Biotinyl-PE—was incorporated into a supported BLM. The biotinylated membrane was then exposed to a solution of streptavidin-Au conjugate, which consisted of 20 nm Au particles labelled with 1 or more streptavidin molecules. Streptavidin is a natural protein that is known to bind very strongly and selectively to the small biotin molecule.

Adsorption of the streptavidin-Au conjugates to the BLMs is exceedingly slow due to the slow diffusion of the 20 nm nanoparticles through the diffusion layer adjacent to the BLM. The diffusion coefficient of a particle with a known hydrodynamic radius, *r*, can be estimated by the Stokes-Einstein relation

$$D\ (\mathrm{m}^2 \cdot \mathrm{s}^{-1}) = \frac{RT}{N_A 6\pi\eta r}, \tag{3}$$

where η is the solvent viscosity.[12] The rate of diffusion-controlled adsorption (i.e. the flux) of a particle with known diffusion coefficient, *D*, can be estimated as follows

$$J\ (\mathrm{mol} \cdot \mathrm{m}^{-2} \cdot s^{-1}) = C\sqrt{\frac{D}{\pi \cdot t}} \tag{4}$$

where *C* is the bulk concentration of the particle in the fluid above the surface and *t* is time.[13] Given the known radius of the streptavidin-Au particles and reasonable values for the concentration of this [precious] material, we can estimate that the adsorption should take between one and a few days at minimum. (In reality, the adsorption will be even slower than this because equation (4) does not take into account the fact that the probability of binding depends on the orientation of the streptavidin-Au conjugate when it approaches the surface.)

The streptavidin-biotin coupling resulted in the deposition of measurable quantities of Au onto the BLM. Figure 4 shows (a) the absorption spectrum of a biotinylated lipid membrane after incubation for 1 week in a suspension of streptavidin-Au conjugate and (b) the absorption spectrum of the [diluted] streptavidin-Au suspension. The peak at 525 nm is due to absorption by surface plasmons in the Au nanoparticles, and gives rise to the red color often observed in Au nanoparticle suspensions. Although the membrane absorption depicted in Figure 4 is easily observed and measured, the peak optical density of approximately 0.002 is rather disappointing given the calculations discussed in section 5.2 above. Given the assumptions described therein, the measured optical density would correspond to a fractional surface coverage of about 1%. Although the absorbance was slightly disappointing, the deposition of a measurable quantity of

metal nanoparticles onto a supported BLM represented a major success. Since the observation of chromatic shifts in these materials should not depend on the overall density of nanoparticles on the surface, this result was adequate to allow for continuation to subsequent phases of the project.

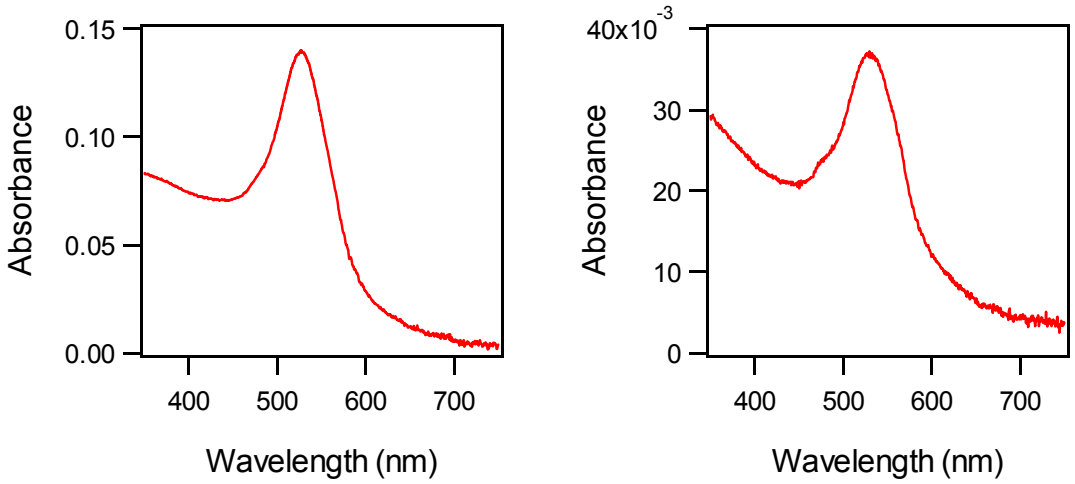

Figure 4. UV-Visible absorption spectra of (a) a suspension of 20 nm Au nanoparticles conjugated to streptavidin., and (b) the streptavidin-Au conjugate bound to a bioniylated BLM.

4.4 Patterning BLMs

By electrophoretically driving the metal nanoparticles against diffusional barriers, we can increase the local concentration of these nanoparticles near the barrier. The region affected by the local concentration increase is expected to be confined very near (within 10 microns or so) the diffusional barriers, depending on a variety of factors such as nanoparticle concentration, the concentration of other ions above the membrane, and the applied voltage gradient. Thus, in order for the nanoparticle redistribution to affect a large fraction of the surface area, the diffusional barriers should be spaced very close together—on the order of tens of microns or less—over a macroscopic area. Following the demonstration of electrophoresis across BLMs and the verifiable binding of metal nanoparticles to these BLMs, we began to work toward microscale patterning of the BLMs in order to achieve a high density of diffusional barriers.

The patterning efforts involved the fabrication of poly(dimethylsiloxane) (PDMS) stamps followed by blotting and stamping of intact BLMs in a manner similar to that used in microcontact printing.[10,14] The stamps were created using a scanning electron microscope calibration grid as the master. The master had a square grid pattern formed from raised lines with a density of 19 mm^{-1}. The square depressions were approximately 50 microns on a side. The

PDMS stamps exhibited the negative of this relief—raised squares approximately 50 microns on a side separated by a gap of several microns.

Patterning was first attempted on BLMs labelled with the Texas Red fluorophore. The results are shown in Figure 5. First, intact membranes were first blotted with the stamp to remove the portion of the membrane contacting the raised squares on the stamp. The grid pattern left behind is shown in Figure 5(a). Next, the stamp was used to stamp the material blotted away onto a freshly-cleaned microscope coverslip. The resulting square pattern is shown in Figure 5(b). From comparison of these two images, it is clear that both the blotting and stamping were partially successful. The blotted membrane shows a definitive square lattice pattern, but it appears that the membrane has been only partially removed by the raised square pads of the PDMS stamp. This is probably due to imperfections in the shape of the stamp. In particular, it appears that the center of the squares may be recessed so that they do not contact the membrane at all. This same defect is repeated in the stamped film shown in Figure 5(b).

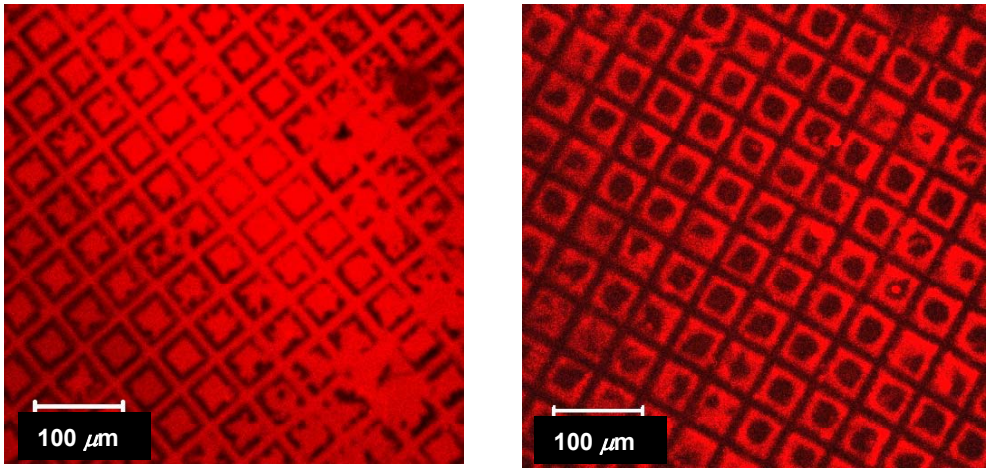

Figure 5. DPPE-TR-labelled BLM (a) blotted and (b) stamped using a PDMS stamp as described above.

The exact shape of the individual membrane pads should not be very important to the success of this work. The inability to perfectly recreate the stamp pattern is at this stage an annoyance, but it does not seem catastrophic to the objective of this work. The primary goal of the stamp-based patterning is to achieve small individual membranes with a high density of diffusional barriers. An important criterion for the success of this stamp-based patterning, however, is the retention of the fluidity of the membrane. After achieving the aforementioned [qualified] success with the patterning, we tested the ability to electrophoretically drive the Texas

Red fluorophore across the individual membrane pads. With only one exception, our many efforts in this area resulted in failure. The motion of the Texas Red fluorophores in these membranes was negligible in the best cases and completely undetectable in the worst. This difficulty remains unresolved at this writing.

4.5 Continuing Work

Work is continuing in my laboratory toward the goals outlined in the original proposal which resulted in the funding of this project. The continued work is being directed away from the BLM systems and toward polymer-based microfluidic systems. Two general strategies are being investigated for the achievement of electrically-stimulated nanoparticle aggregation. The first is the use of "bulk" colloidal suspensions with total volumes of a few microliters. Microfluidic channels molded from plastics or silica are being used in conjunction with charged metal nanoparticles suspended in low dielectric solvents. The second strategy is closely related to the first, but uses polymer microcapsules with volumes on the order of picoliters to contain the colloidal suspensions. This latter strategy is similar to that which has been previously applied to the development of black-and-white "electrophoretic ink."[15]

5. Listing of All Publications and Technical Reports Supplied Under this Contract

(a) Papers published in peer-reviewed journals:

Jie Zheng, Melinda S. Stevenson, Robert S. Hikida, and P. Gregory Van Patten, "Influence of pH on Dendrimer-Protected Nanoparticles," *Journal of Physical Chemistry B* **2002**, *106*, 1252-1255.

(b) Papers published in non-peer-review journals or conference proceedings:

none

(c) Papers presented at meetings, but not published in conference proceedings:

Jie Zheng, M. S. Stevenson, P. Gregory Van Patten, "Regulation of Electronic Coupling and Optical Properties of Dendrimer-Encapsulated Metal Nanoparticles," presented at Materials Research Society Symposium, San Francisco, CA, April 2002.

(d) Manuscripts submitted by not published

none

(e) Technical reports submitted to ARO.

none

6. List of All Participating Scientific Personnel

P. Gregory Van Patten, PI

Jie Zheng, doctoral student (5/31/2001 – 8/31/2001)

Niten Lalpuria, masters student (1/15/2002 – 11/31/2002)

7. Report of Inventions

No inventions or patent disclosures have resulted from this project.

8. Bibliography

1. H. C. van de Hulst, Light Scattering by Small Particles; John Wiley & Sons: New York (1957), Chapters 9, 14.
2. Craig F. Bohren, Donald R. Huffman, Absorption and Scattering of Light by Small Particles; John Wiley & Sons: New York (1983), Chapter 4.
3. Henglein, A. *J. Phys. Chem.* 1993, 97, 5457-5471.
4. Van Patten, P. G.; Stevenson, M. S. *Polym. Mater. Sci. & Eng.* **2001**, *84*, 177-178.
5. Balogh, L.; Valluzzi, R.; Laverduer, K. S.; Gido, S. P.; Hagnauer, G. L.; Tomalia, D. A. *J. Nanoparticle Res.* **1999**, *1*, 353-368.
6. Zhao, M.; Crooks, R. M. *Chem. Mater.* **1999**, *11*, 3379-3385.
7. Esumi, K.; Suzuki, A.; Yamahira, A.; Torigoe, K. *Langmuir* **2000**, *16*, 2604-2608.
8. Zheng, J.; Stevenson, M. S.; Hikida, R. S.; Van Patten, P. G. *J. Phys. Chem. B* **2002**, *106*, 1252-1255.
9. Cremer, P. S.; Boxer, S. G. *J. Phys. Chem. B* **1999**, *103*, 2554-2559.
10. Hovis, J. S.; Boxer, S. G. *Langmuir* **2000**, *16*, 894-897.
11. Link, S.; Wang, Z. L.; El-Sayed, M. A. *J. Phys. Chem. B* **1999**, *103*, 3529-3533.
12. Robert J. Silbey, Robert A. Alberty, Physical Chemistry, 3rd Ed.; John Wiley & Sons: New York (2001), pp. 743-745.
13. Donald T. Sawyer, Andrzej Sobkowiak, Julian L. Roberts, Jr., Electrolchemistry for Chemists, 2nd Ed.; John Wiley & Sons: New York (1995), Chapter 3.
14. Wilbur, J. L.; Kumar, A.; Biebuyck, H. A.; Kim, E.; Whitesides, G. M. *Nanotechnology* **1996**, *7*, 452-457.
15. Comiskey, B.; Albert, J. D.; Yoshizawa, H.; Jacobson, J. *Nature* **1998**, *394*, 253-255.